SIMULATIONS OF SHOCK GENERATION AND PROPAGATION IN LASER-PLASMAS

A.I. Lebo,

Lomonosov Moscow State University, Vorobyevi gori 1, 119234 Moscow, Russia

I.G. Lebo,

Technical University–MIREA, Vernadsky Prospect 78, 119454 Moscow, Russia

D. Batani,

Dipartimento di Fisica "G. Occhialini", Università di Milano Bicocca, Piazza della Scienza 3, 20126 Milano, Italy

Abstract

We analyze the results of a recent experiment performed at the PALS laboratory and concerning ablation pressure at 0.44 μm laser wavelength measured at irradiance up to 2×10^{14} W/cm^2. Using the code "ATLANT", we have performed two-dimensional hydrodynamics simulations. We have compared the simulations with take into account of two equation of state models (QEOS-model and modified Zel'dovich-Raizer model) and have demonstrated rather similar results. The "scaling" of ablation pressure dependence has been got on the base of 2D simulations (for the conditions of PALS-facility experiments).

The short description of experimental set-up.

(see in details: Batani et al. (2003)).

The iodine laser of PALS, which delivers a single beam, 29 cm in diameter, with typical energy of 250 J per pulse at 0.44 μm. The laser pulse is Gaussian in time with a Full Width at Half Maximum (FWHM) of about 400 ps.

The focusing lens had a focal length f = 600 mm (f/2 aperture). A blue filter before the entrance window did cut ω and 2ω light. The diagnostics used to detect the shock breakout from the target rear face consisted in a pair of lenses imaging the rear face onto the slit of a streak camera (Hamamatsu C7700 with S-1 photocathode). The first one was a complex f/2 objective, with f = 100 mm, producing a parallel beam between the two lenses. The second lens had f = 98 cm, giving a total optical magnification M = 9.8.

Stepped targets were made of lathe machining of bulk aluminium. The base was ≈ 8 μm, and the step thickness was d ≈ 8,5 μm. The primary condition of producing high quality flat shocks imposed the use of phase zone plates (PZP). Since, for technical reasons, it was not possible to produce a PZP with the full size of the laser beam, we designed a smaller PZP to be placed at f/2 from target. The design of our optical system (PZP + focusing lens) implied a focal spot had 400 μm FWHM, with a 250 μm flat region in the centre, corresponding to intensities up to 2×10^{14} W/cm^2.

The experimental image allows to measure the time delay between the breakout at the base and at the step, giving the average shock velocity in the step. Velocity of shock wave can be obtained as $D=d/(t_2-t_1)$. Here the time delay between base (t_1) and step (t_2).

The code "ATLANT" (see in details: Lebo&Tishkin, 2006).

$$\frac{d\rho}{dt} = -\rho\vec{\nabla}\vec{v}$$

$$\rho\frac{d\vec{v}}{dt} = -\vec{\nabla}(Z_i \cdot P_E + P_I + P_R) \qquad (7.2)$$

$$Z_i\rho\frac{dE_E}{dt} = -Z_i \cdot P_E\vec{\nabla}\vec{v} + \vec{\nabla}(\kappa_E\vec{\nabla}T_E) - Q_{EI} - Q_{ER} - R_{RAD}(\rho, T_E) + \vec{\nabla}\vec{q}$$

$$\rho\frac{dE_I}{dt} = -P_I\vec{\nabla}\vec{v} + \vec{\nabla}(\kappa_I\vec{\nabla}T_I) + Q_{EI} \qquad (7.3)$$

$$\rho\frac{dE_R}{dt} = -P_R\vec{\nabla}\vec{v} + \vec{\nabla}(\kappa_R\vec{\nabla}T_R) + Q_{ER}$$

$$\left(\frac{\vec{q}}{|\vec{q}|}, \vec{\nabla}\right)\vec{q} = k(\rho, T_E)\cdot\vec{q}$$

$$Q_{EI} = Q_0(\rho, T_E)\frac{T_E - T_I}{T_E^{3/2}}\rho^2$$

$$P_E = P_E(\rho, T_E);\ P_I = P_I(\rho, T_I);\ P_R = P_R(\rho, T_R)$$

$$E_E = E_E(\rho, T_E);\ E_I = E_I(\rho, T_I);\ E_R = E_R(\rho, T_R)$$

Here ρ — density, ν — velocity; E_E, E_I, E_R — specific inner energy of electrons, ion and photons per units of volume; P_E, P_I, P_R, T_E, T_I, T_R— electron, ion and radiation pressures and temperature; E_E, P_E are taken for the unit degree of ionization; R_{RAD} — self radiation losses of plasma; Q_{EI}— is the rate of electron-ion energy exchange in Landau-Spitzer approximation, Q_{ER}— is the rate of electron-photon energy exchange, $\vec{q}$ — is the laser-radiation flux; $\kappa_E, \kappa_I, \kappa_R$ — are the coefficients of thermal conductivity for the electron, ion, and radiation plasma components; Z_i— is the mean degree of ionization in Lagrange cell; k-is the absorption factor of laser radiation.

In our simulations we have neglected radiation transport E_R~0) and used two models of equation of states EOS: 1) a library based on the quotidian equations of state model (QEOS) suggested in (More et al, 1988);

2) improved Zel'dovich&Raiser model (Zel'dovich et al 1966, Afanas'ev et al, 1982), ZRI-model.

Simulation results and comparison with experimental data.

In calculations, we have varied the absorbed laser energy (E_{Las}^{abs}) from 50 to 200 J and the shape of the laser intensity profile ("Flat-top" or "Gauss") while keeping constant the laser wavelength (3ω, λ=0.438 μm) and pulse duration τ_L. For simplicity, the temporal shape of the pulse was taken triangular, beginning at the time t=0, having its maximum at t = 400 ps, and ending at τ_L = 800 ps.

We have simulated the irradiation of 3-layered disks: CH layer (d_{CH}= 2 μm), 1-st Al layer- base (d_{1_Al}=8 μm) and 2-nd Al layer - step (d_{2_Al}=8.5 μm). Fig. 1 shows the initial Lagrangian mesh, $0<r<R_0$. On borders of settlement area (R_0=200 μm) conditions «elastic, thermal isolated walls» have been set. In order to avoid unnecessary numerical problems around the step edge, the base / step profile has been "smoothed" by assuming a sinusoidal profile (over a typical half of wavelength of λ_p=20 μm), as it is clear from Fig. 2.

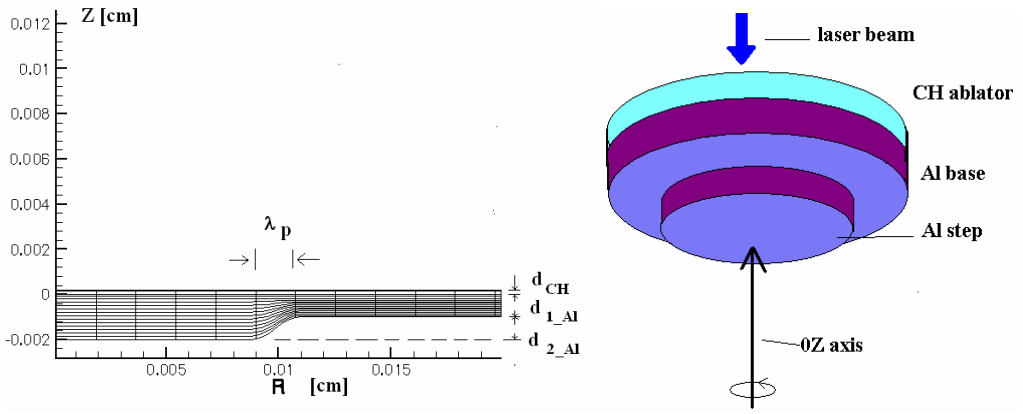

FIG.1 Initial Lagrange mesh used in the ATLANT-code simulation (a). The shapes of target at two time moments, when shock reaches first (b) and second (c) boundaries. E_{Las}^{abs}=100 J (a) The shape of experimental "step target" (b).

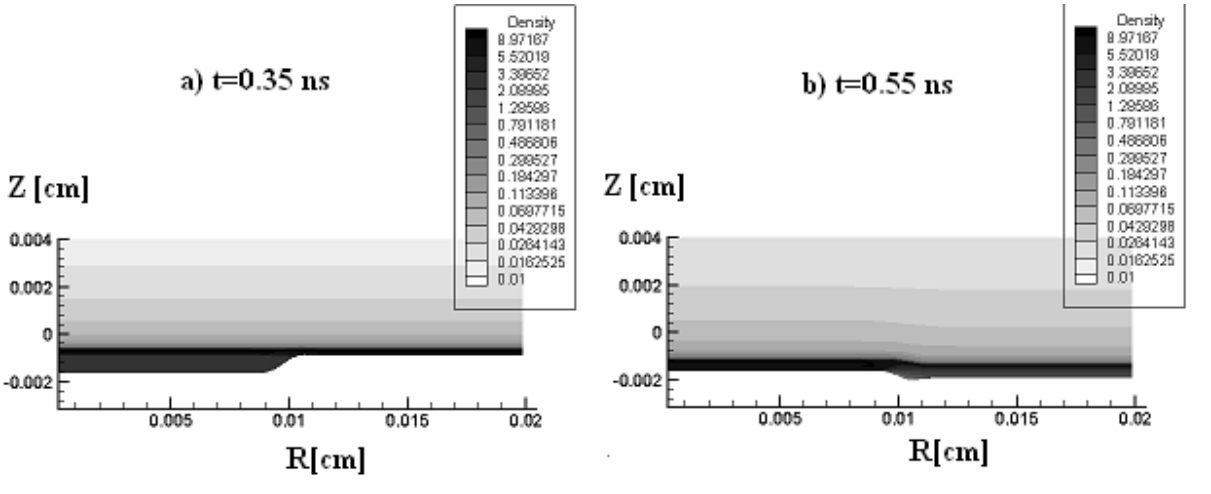

Fig.2 illustrates the comparison of the results of 2D simulations and experimental data ("crosses" in Fig.2). The maximum laser intensity is $I_{\max} = \frac{2 * E_{las}^{abs}}{\pi R_F^2 \tau_L}$, R_F- the radius of focal spot.

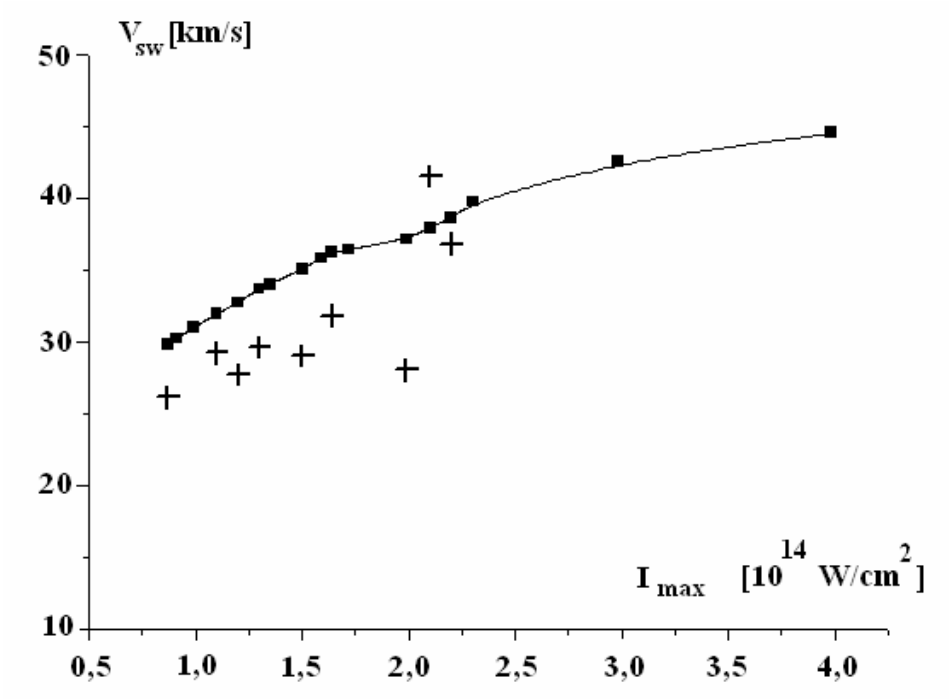

FIG. 2: Shock velocity vs. incident laser intensity, crosses: experimental points after (Batani et al. 2003 a), continuous line: simulations, present work

In our simulations we have supposed of 100% laser energy absorption. In real situation the part of energy is lost. As the result, experimental points are placed some lower.

In the second series of calculations the question on ablation pressure dependence from main laser and target parameters were studied. An Al- layer with initial thicknesses d=20-200 microns without “step profile” was irradiated by the iodine laser. Two-dimensional effects in these calculations were not considered. Calculations have been made for various values of intensity of the laser (I_{max}) at the fixed length of a wave of radiation λ=0,438 μm (results are shown in Fig.3a); and also for lengths of waves λ=0,438, 0,657, 0.876, 1.314 μm (3ω, 2ω, 1.5ω, ω) at fixed maximal intensity $I_{max}=1{,}99\cdot10^{14}$ W/cm^2 (look Fig3b).

Fig.3a demonstrates the results of numerical calculations of dependences of maximum pressure (P_{max}) from intensity at the fixed length of a laser radiation wave λ=0.438 μm (3ω) and Fig3b demonstrates the dependence of P_{max} as function of laser wave length at fixed intensity $I_{max}=1{,}99\cdot10^{14}$ W/cm^2 .

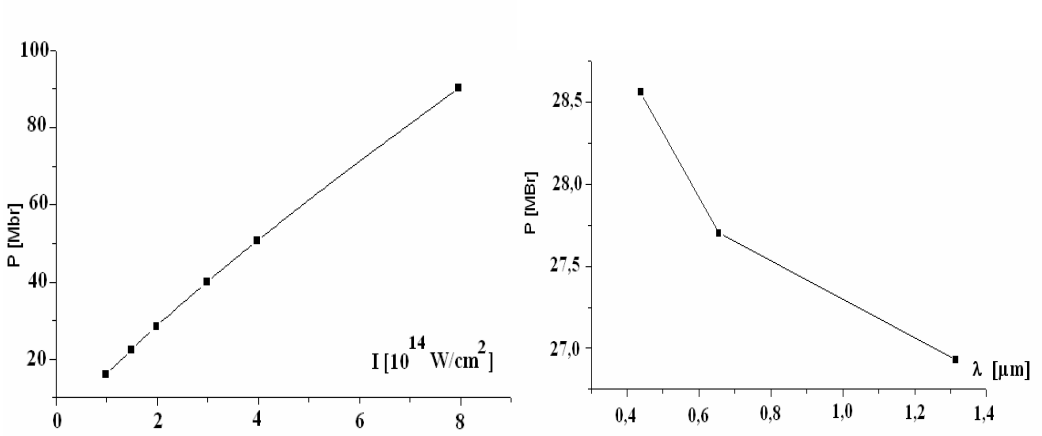

Fig.3. The dependence of pressure on maximum laser intensity (at t=0,4 ns), λ=0.438 μm (a); the dependence of pressure maximum on laser wave length (b) at moment t=0,4 ns

From numerical calculations it is possible to derive the following «scaling»:

$$P_S\,[MBr\,] = 28{,}56 \cdot \left(\frac{I}{1.99 \cdot 10^{14}[W/cm^2]} \right)^{0,83} \cdot \left(\frac{\lambda}{0{,}438[\mu m]} \right)^{-0,05}$$

Fig 4a illustrates the shock wave expansion in condensed aluminum layer along an axis 0Z during the various moments of time extends for the case of QEOS model. Fig.4b illustrates the shock wave expansion for the case of RZI model. Calculations are made for the maximal intensity of laser radiation Imax=1,99 $\cdot 10^{14}$ W/cm^2, lengths of a wave of radiation λ=0.438 μm and d=60 μm .

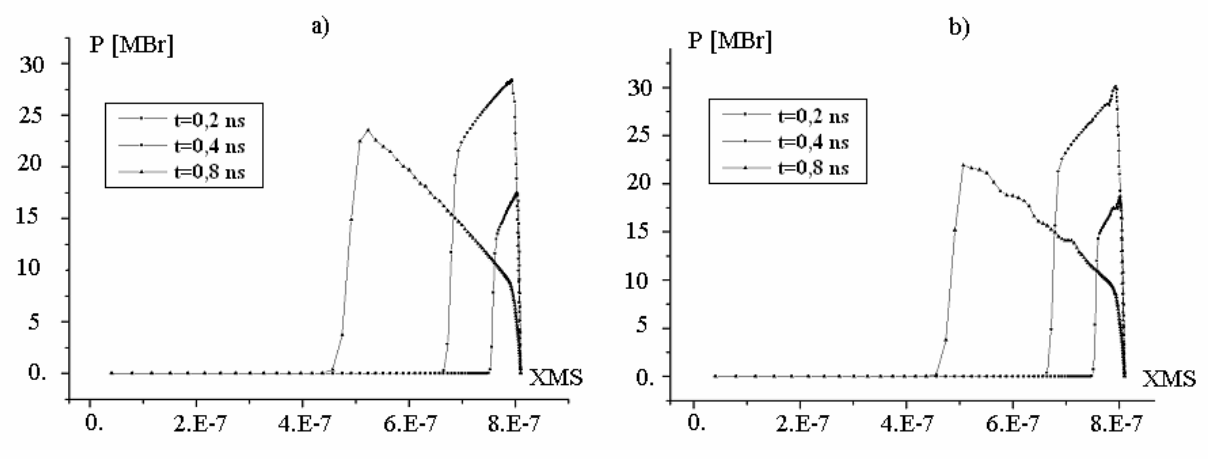

Figure 4. The pressure distribution in the matter as function of mass cords for different time moments: t_1=0,2 ns, t_2=0,4 ns, t_3=0.8 ns a) EOS = QEOS; b) EOS = ZRI model.

The pressure is a function of mass cords. The mass cords: $XMS = \sum_{j=1}^{n} \Delta M_{2j}$ is postponed. Here ΔM_{ij} – the mass of Lagrange cells, (i=2-cells at an axis 0Z), n-number of a cell, where the portion of the absorbed power of laser radiation is defined.

The pressure amplitudes and shock wave velocities in the both models are approximately the same. For example, at the moment t=0,8 ns the maximum of pressure P_{max}=23,5 MBr, mass cords XMS = 0,52·10^{-6} a.u. in the case of QEOS model and P_{max}=22,0 MBr, mass cords XMS = 0,51·10^{-6} a.u in the case of ZRI model (see, Fig.4).

We have made third series of simulations, where laser pulse duration is $\tau=t_3=$ 8 ns (maximal intensity at t_2=4 ns). The range of laser intensities $I_{max}=10^{13}$-$5\cdot10^{14}$ W/см^2, λ=0.438 μm, d=200 μm. Then

$$P_S[MBr] = 28{,}56 \cdot \left(\frac{I}{1.99 \cdot 10^{14}[W/cm^2]}\right)^{0,83} \cdot \left(\frac{\lambda}{0{,}438[\mu m]}\right)^{-0,05} \left(\frac{\tau}{0{,}8[ns]}\right)^{-0,137}$$

The fourth series of simulations has modelled the laser irradiation of targets for different substances: beryllium (Be, Z=4), carbon (C, Z=6), aluminium (Al, Z=13) and silica (Z=14) and corrected formula for P_S:

$$P_S[MBr] = 28{,}56 \cdot \left(\frac{I}{1.99 \cdot 10^{14}[W/cm^2]}\right)^{0,83} \cdot \left(\frac{\lambda}{0{,}438[\mu m]}\right)^{-0,05} \left(\frac{\tau}{0{,}8[ns]}\right)^{-0,137} \left(\frac{Z}{13}\right)^{-0,11}$$

It should notices, that ablation pressure is varied during the target irradiation even for continual intensity (see Caruso, 1968, Mora, 1982). Fig.5 illustrates the results of numerical simulation for laser pulse with rectangular shape with $I_{max}=1{,}99\cdot10^{14}$ W/cm^2 and τ_L = 800 ps , λ=0.438 μm, d=60 μm.

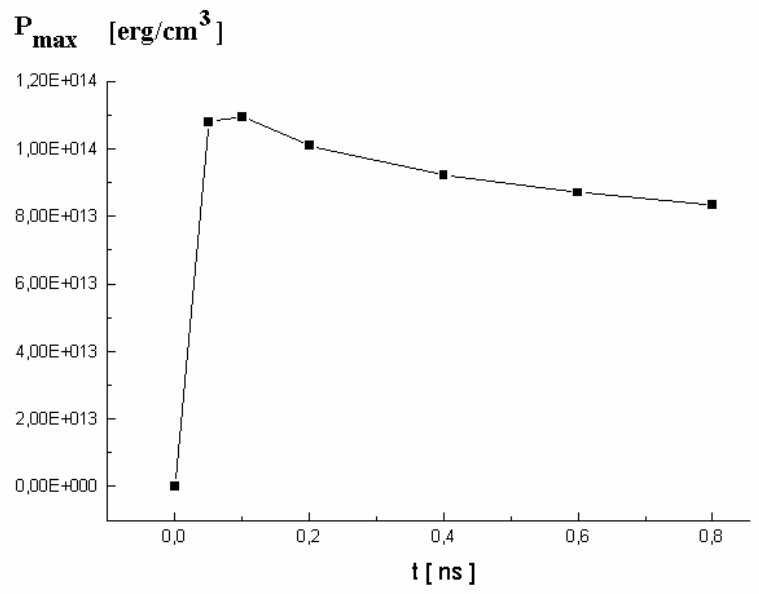

Fig. 5. The dependence of shock pressure from time moments.

.

We have derived some “scaling” from 1D simulations. The accountancy of 2D effects demands on the correction of our relations. We have made a series of 2D simulations of Al foil irradiations: $I(r,t) = I_1(t) \cdot I_2(r)$, where $I_2(r) \sim e^{-(r/R_f)^2}$ (“Gaussian profile”) for two laser wavelengths λ=0.438 μm и λ=1.314 μm, τ_L = 800 ps and three angular shape. E_{las} and R_f have been varied, but $\left(\frac{E_{las}}{R_f^2}\right) = const$. Transverse scale $R_0 = 4R_f$. The maximal pressures (t=0,4 ns) at the axis are shown in Table:

E_{las} [J]	**6,25**	**100**	**400**
R_f [μm]	**50**	**200**	**400**
P[Mbr] (λ=0.438 μm)	**18**	**23**	**26,6**
P[Mbr] (λ=1.314 μm)	**8,6**	**15,8**	**21**

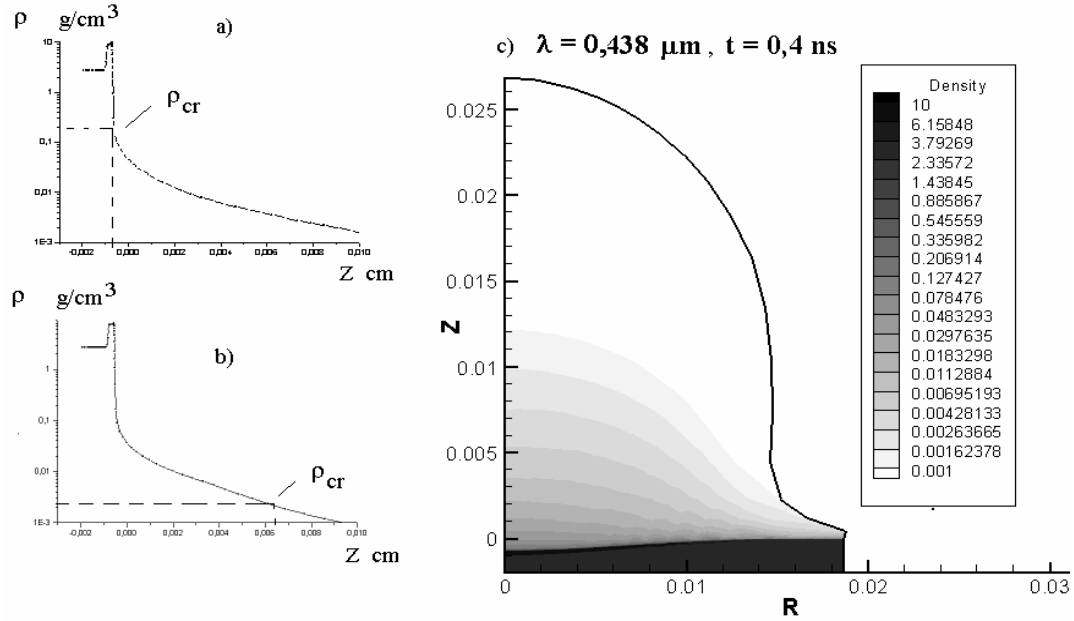

Fig.6. The density distribution along the axis at t=0,4 ns for λ=0.438 μm (a) и λ=1.314 μm (b), ρ_{cr} –critical value. 2D density distribution in plasma plume (c).

Conclusions

1) Our simulations demonstrates good agreement with experimental data, which has been carried out at «PALS» installation;

2) the shock wave rates and jumps of pressure behind of fronts, which have been got from the simulations for two EOS models (QEOS и ZRI), demonstrates approximate results;

3) we have derived the relations of pressure dependence from laser pulse and target parameters in the condition of "PALS" experiments. To our mind, these relations could be useful for planning of the future laser plasma experiments;

4) In the experiments with plane targets the ablation pressure depended on the transverse scale (R_f).

References

Afanas'ev Yu.V., Gamaly E.G., Rozanov V.B. //**Trudi FIAN**, v. 134, p. Moscow, Nauka, (1982)

Batani D., et al., Phys. Rev. E, **63**, 46410 (2001).

Batani D, et al. // **Laser and Particle Beams**, vol. 21, pp. 479-485 (2003).

Batani D et al. // **Physical Review E**, 68, 067403 (2003).

Caruso A. & R. Gratton // **Plasma Phys**., **10**, 867 (1968).

Lebo I.G. et al. // **Laser and Particle Beams**, 22, 267-273, (2004)

Lebo I.G.&Tishkin V.F. Issledovanie gidrodinamicheskoy neustojchivosti v zadachah LTF. // **Monography**, Moscow, FIZMATLIT, (2006)

Mora P. // **Phys. Fluids**, **25**, 1051 (1982).

More R.M. et al. // **Phys. Fluids**, V.31, No.10, p.3059 (1988)

Zel'dovich&Raizer. Fizika udarnih voln I visokotemperaturnih gidrodinamicheskih yavlenij // **Monography**, Moscow, Nauka, FIZMATLIT, 1966.